ELSEVIER

Journal of Alloys and Compounds 444–445 (2007) 369–375

Journal of ALLOYS AND COMPOUNDS

www.elsevier.com/locate/jallcom

Covalency in the f-element–chalcogen bond Computational studies of $[M(N(EPH_2)_2)_3]$ (M = La, U, Pu; E = O, S, Se, Te)

Kieran I.M. Ingram [a], Nikolas Kaltsoyannis [a,*], Andrew J. Gaunt [b], Mary P. Neu [b]

[a] *Department of Chemistry, University College London, 20 Gordon Street, London WC1H 0AJ, UK*
[b] *Inorganic, Isotope and Actinide Chemistry (C-IIAC), Chemistry Division, Los Alamos National Laboratory, Los Alamos, NM 87545, USA*

Received 29 June 2006; received in revised form 26 February 2007; accepted 6 March 2007
Available online 16 March 2007

Abstract

The geometric and electronic structures of the title complexes have been studied using gradient corrected density functional theory. Excellent agreement is observed between computed *r*(M–E) and experimental values in analogous ^{i}Pr complexes. Natural charge analysis indicates that the M–E bond becomes less ionic in the order O > S > S > Te, and that this decrease is largest for U and smallest for La. Natural and Mulliken overlap populations suggest increasing M–E covalency as group 16 is descended, and also in the order La < Pu < U for a given chalcogen. Increased covalency down group 16 arises from increased metal d (and s) participation in the bonding, while that from La to Pu and U stems from larger 5f orbital involvement compared with 4f.

Keywords: Actinide molecules; DFT; Electronic structure; Covalency; Separation

1. Introduction

Ligands capable of extracting An(III) over Ln(III) with a high degree of specificity/selectivity are potentially valuable in the nuclear fuels industry. Key An(III)/Ln(III) pairs with similar ionic radii (and hence similar charge to radius ratios) are very difficult to separate from one another, a desirable goal in many areas including reprocessing spent fuel, storing radiotoxic waste, and transmuting harmful isotopes [1]. Hard donor ligands, such as those bonding through oxygen, have little selectivity for An(III) over Ln(III) ions. However, a greater than 1000-fold preference for An(III) over Ln(III) has been seen when hard oxygen ligands are replaced by softer sulphur-bonding ligands [2].

More recently, experimental work at the Los Alamos National Laboratory has focused on the synthesis and characterisation of a range of homoleptic, trivalent lanthanum and uranium complexes with imidodiphosphinochalcogenide ligands $[N(EPPh_2)_2]^-$ (E = S, Se) [3] and $[N(TeP^iPr_2)_2]^-$ [4]. The principal aim of this research is to explore the differences in f-element–ligand bonding as the donor atoms progress from hard to soft, with the anticipation that the uranium–heavier chalcogen bond will be more covalent than the analogous lanthanum bond. Structural data suggest that this is indeed the case, with significantly shorter *r*(U–Te) than *r*(La–Te), despite the ionic radii of La^{3+} and U^{3+} being essentially identical.

In this contribution we report the initial results of our computational studies of these systems, and address the structures, partial charges and electronic populations in $[M(N(EPH_2)_2)_3]$ (M = La, U; E = O, S, Se, Te), models for the experimentally characterised ^{i}Pr systems. We have also extended the computational work to the Pu systems, as very recent work at Los Alamos has furnished imidodiphosphinochalcogenide complexes of this element [5], and we wished to compare the metal–ligand bonding in analogous La(III), U(III), and Pu(III) compounds.

2. Computational details

All calculations were carried out using gradient corrected density functional theory, as implemented in the Gaussian '03

* Corresponding author.
E-mail address: n.kaltsoyannis@ucl.ac.uk (N. Kaltsoyannis).

0925-8388/$ – see front matter © 2007 Elsevier B.V. All rights reserved.
doi:10.1016/j.jallcom.2007.03.048

(G03) [6] and Amsterdam Density Functional (ADF) [7–9] quantum chemical codes. Spin-unrestricted calculations were performed on all uranium and plutonium complexes to account for the formal f^3/f^5 configurations of U(III) and Pu(III), respectively; La is formally f^0 and therefore spin restricted calculations were performed.

2.1. G03

The GGA functional PBE [10,11] was used for all G03 calculations. (14s 13p 10d 8f)/[10s 9p 5d 4f] segmented valence basis sets with Stuttgart–Bonn variety [12] relativistic effective core potentials (RECPs) were used for uranium and plutonium, and a (14s 13p 10d 8f)/[10s 8p 5d 4f] segmented valence basis set with a Stuttgart–Bonn RECP [12] was used for lanthanum. 6-31G* basis sets were used for the O, S, Se, N, and P atoms, and the smaller 6-31G was used for H. Te was described with a (4s 5p)/[2s 3p] Stuttgart basis set [13] augmented to (4s 5p 7d)/[2s 3p 3d] with STO-3G* [14,15] polarisation functions (for consistency, as 6-31G* includes polarisation functions on O, S, and Se); a Stuttgart RECP was also used for Te [13]. The validity of this augmented Te basis set was checked by constructing an analogous Se basis set – a Stuttgart (4s 5p)/[2s 3p] augmented to (4s 5p 4d)/[2s 3p 2d] – and performing test geometry optimisations on $[M(N(SePH_2)_2)_3]$ for M = La, U; similar geometries were found with both methods. The default values for the integration grid (fine) and the convergence criteria were used for all lanthanum and uranium geometry optimisations (maximum force $= 4.5 \times 10^{-4}$ a.u. Å^{-1}, SCF $= 10^{-8}$). The plutonium calculations were more problematic and the following convergence criteria were achieved: $[Pu(N(OPH_2)_2)_3]$ (maximum force $= 7 \times 10^{-4}$ a.u. Å^{-1}, SCF $= 10^{-7}$), $[Pu(N(SPH_2)_2)_3]$ (maximum force $= 8 \times 10^{-4}$ a.u. Å^{-1}, SCF $= 10^{-5}$), $[Pu(N(SePH_2)_2)_3]$ (maximum force $= 5 \times 10^{-4}$ a.u. Å^{-1}, SCF $= 10^{-8}$), $[Pu(N(TePH_2)_2)_3]$ (maximum force $= 8 \times 10^{-4}$ a.u. Å^{-1}, SCF $= 10^{-5}$). A natural charge and population analysis [16–22] was carried out on all G03 optimised structures.

Little spin contamination was found for the quadruplet U(III) complexes, as evidenced by the fact that the values of $\langle S^2 \rangle$ were close to 3.75 in all cases, with 3.77 for $[U(N(TePH_2)_2)_3]$ being the largest deviation from the ideal. Spin contamination in the plutonium complexes is more significant than in the uranium complexes, however the largest $\langle S^2 \rangle$ calculated was 8.865 ($[Pu(N(TePH_2)_2)_3]$), not a significant deviation from the ideal 8.75.

2.2. ADF

Single point calculations on optimised G03 structures were carried out in ADF. As with G03 the PBE functional was used. TZP zero order regular approximation (ZORA) basis sets were used for each of the f-elements together with DZP ZORA basis sets for O, S, Se, P, and N; DZ was used for H. ADF does not have a DZP basis set for Te and so TZP polarisation functions were added to the DZ basis. The frozen core approximation was used. A 5d core was used for U and Pu, 4d for La and Te, 3d for Se, 2p for S, P, and 1s for O, N. A Mulliken overlap population [23,24] analysis was carried out.

2.3. Ligand models and point group symmetry

Experimentally the phosphorus-bound R group is *iso*-propyl. However the use of such R groups in the calculations is extremely time-consuming, and so to cut computational cost we tested two approximations by replacing ^{i}Pr with H and Me. Extensive tests (data not shown here) on the energies, bond lengths, and charges of these complexes revealed that the choice of R group does not affect the metal–chalcogen bond lengths or charges to any significant extent. We also tested the validity of idealising the geometries to the D_3 symmetry group (with its favourable consequences for electronic structure analysis), and again concluded that this has little impact upon the quality of the results. Thus the present paper focuses on studies of the title complexes in the D_3 point group.

3. Results

3.1. Geometries

Crystallographic data for the structures of $[M(N(SP^iPr_2)_2)_3]$ and $[M(N(SeP^iPr_2)_2)_3]$ (M = La, U) provided the initial conformations for the geometry optimisations [5]. The ^{i}Pr fragments were replaced with H, the structures idealised to D_3, and geometry optimisations were carried out on the four complexes obtained. Pu structures were then constructed by substituting Pu into the optimised uranium structures and re-optimising. Finally, starting structures for the oxygen- and tellurium-donor ligand calculations were constructed from these optimised structures by substituting S by O for each metal and Se by Te. A total of 12 D_3 geometry optimised structures were achieved: $[M(N(EPH_2)_2)_3]$ with E = O, S, Se, Te and M = La, U, Pu.

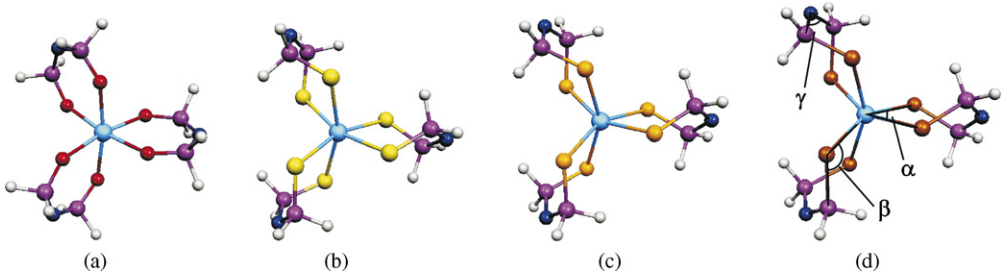

Fig. 1. Ball and stick representations of the D_3 optimised geometries of $[La(N(EPH_2)_2)_3]$; E = O (a), S (b), Se (c), and Te (d).

Table 1
Selected bond lengths and angles (see Fig. 1(d) for definitions of α, β, γ) from the optimised geometries of our target molecules, together with experimental data in italics (from Ref. [4])

	Lanthanum				Uranium				Plutonium			
	O	S	Se	Te	O	S	Se	Te	O	S	Se	Te
Bond lengths (Å)												
M–E	2.417	2.916	3.027	3.232 (*3.224*)	2.393	2.849	2.955	3.126 (*3.164*)	2.364	2.83	2.932	3.135
P–E	1.553	2.043	2.198	2.443 (*2.445*)	1.555	2.048	2.206	2.461 (*2.438*)	1.555	2.044	2.202	2.451
P–N	1.612	1.634	1.639	1.642 (*1.594*)	1.612	1.636	1.638	1.643 (*1.586*)	1.611	1.635	1.639	1.643
Bond angles (°)												
E–M–E (α)	80.5	87.0	90.1	92.7 (*90.9*)	81.7	89.4	91.3	92.1 (*90.9*)	82.9	88.2	90.5	92.1
P–E–M (β)	135.6	107.5	102.8	99.0 (*111.1*)	134.3	105.9	103.4	101.8 (*111.7*)	134.3	107.6	104.5	101.3
N–P–E (γ)	119.9	121.3	121.4	121.2 (*120.8*)	120.0	120.8	121.5	120.4 (*120.4*)	120.0	120.8	121.0	120.5

Fig. 1 shows ball + stick representations of the structures of $[La(N(EPH_2)_2)_3]$, and the corresponding U and Pu structures (not shown) are similar. Selected bond lengths and bond angles are given in Table 1, and Fig. 2 illustrates r(M–E) down group 16 for all three metals. Fig. 2 shows that as the chalcogen is changed from oxygen to tellurium, r(M–E) lengthens significantly, the increase being largest between oxygen and sulphur, followed by a smaller increase from sulfur through selenium to tellurium. In addition to those given in Ref. [4], crystallographic data are available for $[M(N(EPH_2)_2)_3]$ (E = S; M = La, U, Pu and E = Se; M = La, U) [5]. The calculated r(M–E) agree very well with experiment in all cases—the maximum discrepancy between theory and experiment is *ca.* 0.04 Å.

Fig. 2 shows that while r(M–O) is similar for all three metals, the difference between r(La–E) and r(An–E) increases down group 16. Fig. 3 emphasises this point by normalising r(M–O) to zero for each of the metals. In this figure we see clearly that while r(U–E) increases as the chalcogen becomes heavier, r(Pu–E) increases slightly more steeply, and r(La–E) considerably more steeply. Thus while r(La–O) is *ca.* 0.02 Å longer than r(U–O) and *ca.* 0.05 Å longer than r(Pu–O) (as would be expected as Pu^{3+} has a smaller ionic radius than the other two metals), r(La–Te) is *ca.* 0.10 Å longer than r(Pu–Te) and *ca.* 0.11 Å longer than r(U–Te). This result agrees well with experiment, and suggests that U–E and Pu–E bonding for the heavier chalcogens is indeed somewhat different from that in the analogous La complexes. This is probed further in Sections 3.2–3.4.

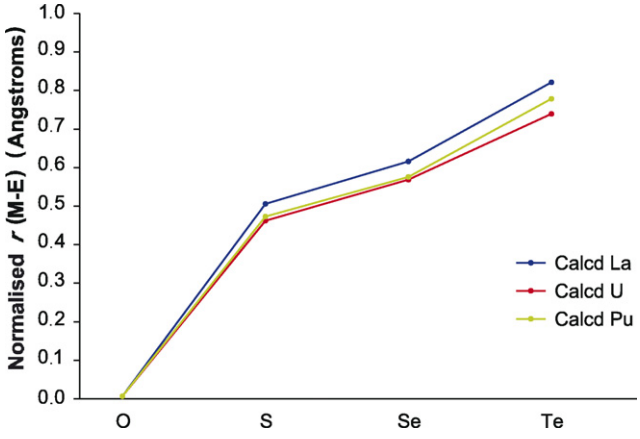

Fig. 3. Normalised calculated r(M–E) in $[M(N(EPH_2)_2)_3]$ for M = La, U, Pu; E = O, S, Se, Te, at the optimised structures. r (M–O) has been set to zero for each metal.

Fig. 4 illustrates the increase in r(P–E) as group 16 is descended. La, U and Pu have similar r(P–E) in the oxygen and sulphur complexes. A large increase in r(P–E) is seen between the O and S complexes, and smaller increases in r(P–E) are found from S to Se and Te. While r(M–E) is shorter for M = An than La (for a given E), r(P–E) is longer. This effect is not large,

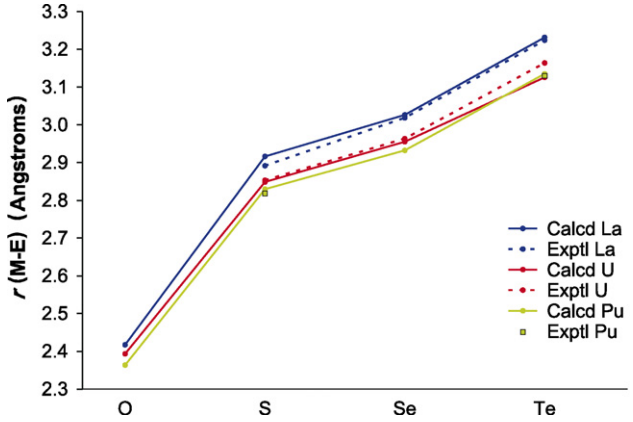

Fig. 2. Calculated r(M–E) in $[M(N(EPH_2)_2)_3]$ for M = La, U, Pu; E = O, S, Se, Te, at the optimised structures together with experimental data.

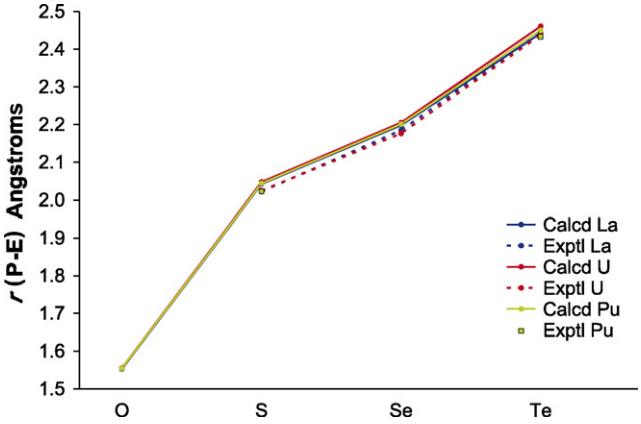

Fig. 4. Calculated r (P–E) in $[M(N(EPH_2)_2)_3]$ for M = La, U, Pu; E = O, S, Se, Te, at the optimised structures together with experimental data.

∼ 0.01 Å, but it is present consistently, possibly suggesting that enhanced U–E (and Pu–E to a lesser extent) bonding occurs at the expense of the P–E bonding within the ligands.

The P–N bond lengths are not reproduced perfectly by our calculations; a systematic overestimation of *ca.* 0.05 Å is present. While this discrepancy is larger that we would like, it is not a major concern, particularly given the generally excellent agreement between theory and experiment for the M–E distances.

The ∠EME bite angles α, as defined in Fig. 1(d), agree well with experimental results for all three metals. More specifically, the correct trend is seen; as the chalcogen gets bigger so too does ∠EME. Once again a large jump is seen on moving from O to S, and then a smaller gradual increase from S through Se to Te. The ∠NPE angle is essentially constant in all the complexes, barely deviating from 120°. The ∠PEM angle is underestimated computationally by *ca.* 10°. The reasons for this are unclear, but as when considering *r*(P–N), we do not believe that these minor angular deviations will adversely affect our analyses of the M–E bonding.

3.2. Natural charge analysis of $[M(N(EPH_2)_2)_3]$ for M = La, U, Pu; E = O, S, Se, Te

The natural charges for selected atoms are collected in Table 2 and Fig. 5. For lanthanum we calculate a decrease in q_{La} from 2.490 (O) to 1.834 (Te), a drop of 0.656, accompanied by an increase in $q_{E_{La}}$ from −1.174 (O) to −0.494 (Te), a rise of 0.680. For uranium we calculate a decrease in q_U from 2.218 (O) to 1.524 (Te), a drop of 0.694, accompanied by an increase in q_{E_U} from −1.132 (O) to −0.444 (Te), an increase of 0.688. The results for plutonium show charges on both M and E_{Pu} in between those seen for La and U; a decrease in q_{Pu} from 2.287 (O) to 1.615 (Te), a drop of 0.672, accompanied by an increase in $q_{E_{Pu}}$ from −1.143 (O) to −0.458 (Te), a rise of 0.685.

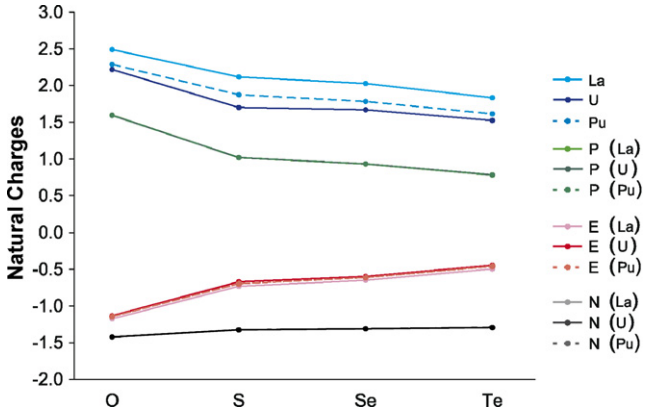

Fig. 5. Natural charges of $[M(N(EPH_2)_2)_3]$ for M = La, U, Pu; E = O, S, Se, Te at the optimised geometries.

For all metals, a decrease of ∼ 0.81 for q_P and a small rise of 0.13 for q_N is seen on descending the chalcogens.

Comparison of the metal charges shows that $q_{La} > q_{Pu} > q_U$ in $[M(N(EPH_2)_2)_3]$ for all E. In the S, Se, and Te complexes q_{La} is *ca.* 22% larger than q_U, but it is only 12% larger with E = O; similarly q_{La} is *ca.* 15% larger than q_{Pu} for all complexes except $[M(N(OPH_2)_2)_3]$, where is it 9% larger. In addition, q_{E_M} in $[La(N(EPH_2)_2)_3]$ is typically *ca.* 10% more negative than in $[U(N(EPH_2)_2)_3]$ or *ca.* 7% more negative than in $[Pu(N(EPH_2)_2)_3]$, with $[M(N(OPH_2)_2)_3]$ once again being the exception with a difference between $q_{O_{La}}$ and q_{O_U} of 4%, and a difference between $q_{O_{La}}$ and $q_{O_{Pu}}$ of 3%.

In summary, q_{La} is more positive than q_U, and $q_{E_{La}}$ is more negative than q_{E_U} for a given E. The calculated values of q_{Pu} and $q_{E_{Pu}}$ fall in between those calculated for La and U. All three q_M become less positive as the chalcogen attached to them becomes heavier; all q_E are progressively less negative for the heavier chalcogens.

Table 2
Natural charges of $[M(N(EPH_2)_2)_3]$ M = La, U, Pu; E = O, S, Se, Te at the optimised geometries

Atom	Natural charges (q_{Nat})				Δ(O − Te)
	O	S	Se	Te	
La	2.490	2.117	2.027	1.834	0.656
E_{La}	−1.174	−0.731	−0.649	−0.494	−0.680
P_{La}	1.596	1.018	0.929	0.779	0.817
N_{La}	−1.424	−1.327	−1.312	−1.293	−0.131
$\Delta(q_{Nat\,La} - q_{Nat\,E_{La}})$	3.664	2.848	2.675	2.327	
U	2.218	1.701	1.670	1.524	0.694
E_U	−1.132	−0.670	−0.597	−0.444	−0.688
P_U	1.592	1.017	0.932	0.782	0.811
N_U	−1.421	−1.323	−1.308	−1.289	−0.132
$\Delta(q_{Nat\,U} - q_{Nat\,E_U})$	3.350	2.371	2.267	1.968	
Pu	2.287	1.873	1.781	1.615	0.672
E_{Pu}	−1.143	−0.695	−0.612	−0.458	−0.685
P_{Pu}	1.595	1.018	0.931	0.780	0.815
N_{Pu}	−1.423	−1.323	−1.309	−1.291	−0.132
$\Delta(q_{Nat\,Pu} - q_{Nat\,E_{Pu}})$	3.430	2.569	2.393	2.072	

Table 3
Natural population data for M in [M(N(EPH$_2$)$_2$)$_3$] M = La, U, Pu; E = O, S, Se, Te at the optimised geometries

Species	Lanthanum				Uranium				Plutonium			
	O	S	Se	Te	O	S	Se	Te	O	S	Se	Te
Natural totals												
s	0.12	0.28	0.34	0.42	0.16	0.36	0.43	0.51	0.17	0.37	0.44	0.50
p	0.01	0.01	0.01	0.02	0.01	0.01	0.01	0.01	0.01	0.01	0.01	0.02
d	0.19	0.41	0.46	0.57	0.17	0.35	0.43	0.62	0.17	0.34	0.38	0.48
f	0.23	0.20	0.18	0.16	3.33	3.47	3.38	3.29	5.35	5.38	5.37	5.36

As shown in Table 2 and Fig. 5, the natural charge difference between M and E_M decreases as E becomes heavier. The significant reduction in the M–E charge difference between E = O and E = Te for all three metals suggests that the M–E bond becomes significantly less polar as the O → Te group is descended. The natural analysis scheme gives a 36.5% reduction in $\Delta(q_{La} - q_{E_{La}})$ from O to Te, a 41.3% reduction in $\Delta(q_U - q_{E_U})$ and a 39.6% decrease in $\Delta(q_{Pu} - q_{E_{Pu}})$, suggesting that the decrease in ionicity as the chalcogens are descended is greatest in U–E and smallest in La–E.

3.3. Natural population analysis

Table 3 and Fig. 6 present the natural population analysis data for all [M(N(EPH$_2$)$_2$)$_3$].

The data show that the s-populations increase as group 16 is descended for all metals, with the two actinide complexes showing a slightly larger increase. The natural p-populations are very close to the formal $(n-1)p^6$ for all metals, and no change is seen in the p-populations on moving from E = O to Te.

The metallic f-populations are somewhat larger than the formal f^0, f^3 and f^5 values for La, U, and Pu, respectively, the difference being systematically larger for the uranium and plutonium complexes. There is no definite increase/decrease in f-population as the chalcogens are descended, but there is a trend towards a small decrease from S to Te.

In all cases, the metal d-populations increase from E = O to Te; for U this is from 0.17 (O) to 0.62 (Te), while for La a smaller d-population increase is observed (0.19 (O)–0.57 (Te)). Interestingly, the d-population increase is smallest for the plutonium complexes—0.17 (O)–0.48 (Te).

The overall conclusion from the natural population data is that for each of the La, U, and Pu families of complexes, as group 16 is descended electron density enters the $(n-1)$d levels, and to a lesser extent the ns levels (except for Pu, where the increase in n s-population is comparable with the $(n-1)$d). The net amount of charge transferred to U on moving from E = O to E = Te is greatest (0.76e$^-$) and to La is the least (0.62e$^-$), with Pu in between (0.66e$^-$).

Thus natural population analysis suggests that the covalent contribution to the M–E interaction increases as the chalcogens are descended. In addition, the data suggest that this covalency increases more steeply for uranium than for lanthanum, with plutonium falling somewhere between the other two metals. While the covalent contribution to La–O, U–O, and Pu–O is of a similar magnitude, the covalent component of U–Te is larger than that of Pu–Te, which in turn is larger than that of La–Te.

The population data also indicate that, while the f-orbitals play a role in bonding between M and E, the principal reason for increased covalency in M–Te over M–O is enhanced d participation. The f-orbitals are, however, partially responsible for the difference between U–E/Pu–E and La–E for any given E, indicated by the larger f-populations of U/Pu compared with the formal f^3/f^5 configuration versus the less significantly increased f-populations of La compared with the formal f^0 configuration.

3.4. Mulliken overlap populations

The Mulliken overlap populations are reported in Table 4 and illustrated in Fig. 7. A significant increase in overlap population is seen down group 16 for the lanthanum, uranium, and plutonium complexes. For both M–E and M^{3+}–L^{3-}, this increase is

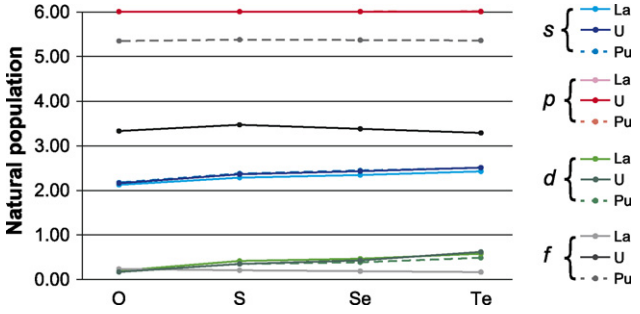

Fig. 6. Natural populations of [M(N(EPH$_2$)$_2$)$_3$] M = La, U, Pu; E = O, S, Se, Te at the optimised geometries.

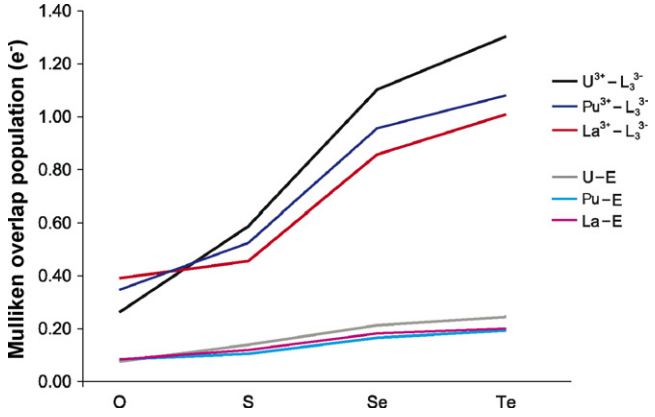

Fig. 7. Selected Mulliken overlap populations in [M(N(EPH$_2$)$_2$)$_3$] M = La, U, Pu; E = O, S, Se, Te at the optimised D_3 geometries.

Table 4
Selected Mulliken overlap populations in $[M(N(EPH_2)_2)_3]$ M = La, U, Pu; E = O, S, Se, Te at the optimised D_3 geometries

	Lanthanum				Uranium				Plutonium			
	O	S	Se	Te	O	S	Se	Te	O	S	Se	Te
M–E	0.08	0.10	0.17	0.19	0.08	0.14	0.21	0.24	0.08	0.10	0.16	0.18
M^{3+}–L^{3-}	0.39	0.46	0.86	1.01	0.26	0.59	1.10	1.30	0.35	0.53	0.96	1.08

largest for U. However whilst the M^{3+}–L^{3-} overlap population is considerably larger for Pu than La in each of the three heavier chalcogen complexes, the M–E overlaps are similar for the two metals.

Mulliken overlap populations can be considered as the number of electrons covalently bonding between two atoms, and hence the data suggest enhanced covalency in the compounds of the heavier chalcogens. Furthermore the data show a clear ordering of U > Pu > La regarding increased covalency in analogous metal complexes for a given E (E = S, Se, Te).

4. Conclusions

In this contribution we have reported DFT studies of the series of complexes $[M(N(EPH_2)_2)_3]$ M = La, U, Pu; E = O, S, Se, Te. The principal conclusions are:

(i) In general, very good agreement between theoretical and experimental geometries is found. In particular, the experimental observation that metal–chalcogen distances in analogous La and An (An = U, Pu) complexes with S-, Se-, and Te-donor ligands are shorter in the actinide systems, is reproduced computationally. Furthermore, the difference between *r*(La–E) and *r*(An–E) is larger for the heavier E, again agreeing with experimental data. Fig. 3 is particularly pleasing, showing that the lengthening of M–E as group 16 is descended increases in the order U < Pu < La.
(ii) The natural charge analysis reveals a significant reduction in the M–E charge difference between E = O and E = Te, suggesting the M–E bond becomes less ionic as group 16 is descended. Furthermore, the decrease in ionicity is greatest in U–E and smallest in La–E, with Pu–E in between.
(iii) Natural population analysis and Mulliken overlap populations both point towards a greater metal participation in M–E bonding as group 16 is descended, suggesting increased covalency between the metals and the heavier chalcogens. Furthermore, the data indicate greater covalency in U–E than in Pu–E, and greater covalency in Pu–E than in La–E.

Our conclusions are similar to those of Roger et al. [25] who probed the M–S bonding in $[Ce(Cp^*)_2(dddt)]^-$ and $[U(Cp^*)_2(dddt)]^-$,[25] (dddt = 5,6-dihydro-1,4-dithiin-2,3-dithiolate). They found the actinide compounds to have significantly shorter M–S bonds, as well as decreased M–S charge differences and increased M–S overlap populations, and concluded that uranium has a more covalent interaction with S than cerium does.

We are currently expanding this study to include an analysis of the valence molecular orbital structure of the title complexes, as well as a bond energy decomposition using the Ziegler–Rauk approach [26,27]. We are also extending the range of metals to include Ce, Pr, Pm, Eu, and Lu among the lanthanides, and Np, Am, Cm, and Lr in the 5f series. The results of these studies will be reported in future papers.

Acknowledgements

We are grateful to the UK EPSRC for a studentship to KIMI, and for computing resources under grant GR/S06233/01.

References

[1] http://www.world-nuclear.org/info/inf69.htm.
[2] M.P. Jensen, A.H. Bond, J. Am. Chem. Soc. 124 (2002) 9870.
[3] A.J. Gaunt, B.L. Scott, M.P. Neu, Chem. Commun. 255 (2005) 3215.
[4] A.J. Gaunt, B.L. Scott, M.P. Neu, Angew. Chem. Int. Ed. 45 (2006) 1638.
[5] A.J. Gaunt, unpublished results.
[6] Gaussian '03, Revision C.02, M.J. Frisch, G.W. Trucks, H.B. Schlegel, G.E. Scuseria, M.A. Robb, J.R. Cheeseman, J.A. Montgomery Jr., T. Vreven, K.N. Kudin, J.C. Burant, J.M. Millam, S.S. Iyengar, J. Tomasi, V. Barone, B. Mennucci, M. Cossi, G. Scalmani, N. Rega, G.A. Petersson, H. Nakatsuji, M. Hada, M. Ehara, K. Toyota, R. Fukuda, J. Hasegawa, M. Ishida, T. Nakajima, Y. Honda, O. Kitao, H. Nakai, M. Klene, X. Li, J.E. Knox, H.P. Hratchian, J.B. Cross, V. Bakken, C. Adamo, J. Jaramillo, R. Gomperts, R.E. Stratmann, O. Yazyev, A.J. Austin, R. Cammi, C. Pomelli, J.W. Ochterski, P.Y. Ayala, K. Morokuma, G.A. Voth, P. Salvador, J.J. Dannenberg, V.G. Zakrzewski, S. Dapprich, A.D. Daniels, M.C. Strain, O. Farkas, D.K. Malick, A.D. Rabuck, K. Raghavachari, J.B. Foresman, J.V. Ortiz, Q. Cui, A.G. Baboul, S. Clifford, J. Cioslowski, B.B. Stefanov, G. Liu, A. Liashenko, P. Piskorz, I. Komaromi, R.L. Martin, D.J. Fox, T. Keith, M.A. Al-Laham, C.Y. Peng, A. Nanayakkara, M. Challacombe, P.M.W. Gill, B. Johnson, W. Chen, M.W. Wong, C. Gonzalez, J.A. Pople, Gaussian Inc., Wallingford, CT, 2004.
[7] ADF2004.01, SCM, Theoretical Chemistry, Vrije Universiteit, Amsterdam, The Netherlands, http://www.scm.com.
[8] G. te Velde, F. Bickelhaupt, S. van Gisbergen, C.F. Guerra, E. Baerends, J. Snijders, T. Ziegler, J. Comput. Chem. 22 (2001) 931.
[9] C.F. Guerra, J. Snijders, G. te Velde, E. Baerends, Theor. Chem. Acc. 99 (1998) 391.
[10] J.P. Perdew, K. Burke, M. Ernzerhof, Phys. Rev. Lett. 77 (1996) 3865.
[11] J.P. Perdew, K. Burke, M. Ernzerhof, Phys. Rev. Lett. 78 (1997) 1396.
[12] X. Cao, M. Dolg, J. Mol. Struct. (Theochem) 673 (2004) 203.
[13] A. Bergner, M. Dolg, W. Kuechle, H. Stoll, H. Preuss, Mol. Phys. 80 (1993) 1431.
[14] W.J. Hehre, R.F. Stewart, J.A. Pople, J. Chem. Phys. 59 (1969) 2657.
[15] J.B. Collins, P.V.R. Schleyer, J.S. Binkley, J.A. Pople, J. Chem. Phys. 64 (1976) 5142.
[16] J.E. Carpenter, F. Weinhold, J. Mol. Struct. (Theochem) 169 (1988) 41.
[17] J.E. Carpenter, PhD Thesis, University of Wisconsin, Madison, WI, 1987.

[18] J.P. Foster, F. Weinhold, J. Am. Chem. Soc. 102 (1980) 7211.
[19] A.E. Reed, F. Weinhold, J. Chem. Phys. 78 (1983) 4066.
[20] A.E. Reed, R.B. Weinstock, F. Weinhold, J. Chem. Phys. 83 (1985) 735.
[21] A.E. Reed, L.A. Curtiss, F. Weinhold, Chem. Rev. 88 (1988) 899.
[22] F. Weinhold, J.E. Carpenter, The Structure of Small Molecules and Ions, Plenum, 1988, p. 227.
[23] P. Politzer, R.S. Mulliken, J. Chem. Phys. 55 (1971) 5135.
[24] D.L. Grier, J.A. Streitwieser, J. Am. Chem. Soc. 104 (1982) 3556.
[25] M. Roger, L. Belkhiri, P. Thuéry, M. Arliguie, A. Fourmigué, M. Boucekkine, M. Ephritikine, Organometallics 24 (2005) 4940.
[26] T. Ziegler, A. Rauk, Theor. Chim. Acta 46 (1977) 1.
[27] T. Ziegler, A. Rauk, Inorg. Chem. 18 (1979) 1558.